Electric Field Probes—A Review

HOWARD I. BASSEN, SENIOR MEMBER, IEEE, AND GLENN S. SMITH, SENIOR MEMBER, IEEE

Abstract—**Electric field probes consisting of a dipole antenna, RF detector, nonperturbing transmission line, and readout device have been implemented in a variety of ways. Three orthogonal dipoles are generally used in an *E*-field probe to provide a response which is nearly isotropic for all polarizations of the incident field. Diode detectors have been used with electrically short or resistivity loaded dipoles to produce very broadband devices (0.2 MHz to 26 GHz). Thermocouple detectors are used to provide true time-averaged data for high peak-power modulated fields. Optical fibers, together with a suitably modulated light source, may be used to form a wide-band nonperturbing data link from the dipole and detector to a remote readout. Application of *E*-field probes range from the measurement of fields in living animals exposed to nonionizing radiation to the measurement of fields in air for electromagnetic compatability or radiation safety purposes. Probes are available that can measure field strengths from less than 1 V/m to over 1000 V/m (rms).**

INTRODUCTION

FOR MANY YEARS electric fields have been measured in air and in material media using electric field probes. The term "*E*-field probe" will be used to describe a variety of measurement tools with the following basic characteristics: a dipole antenna with a detector mounted across the gap which separates the two arms of the dipole, a nonperturbing data link connecting the detector output with a remote observation site, and the ability to measure accurately field strengths from about 1 V/m to 1000 V/m (rms). Three mutually perpendicular, single-antenna, *E*-field probes may be combined in a closely spaced array to construct a probe with an isotropic response.

Early versions of the *E*-field probe were usually "homemade" one-of-a-kind devices used to measure relative field distributions, such as the field in the aperture of a microwave antenna [1]. When concern arose over the possible health hazards of nonionizing electromagnetic radiation and government safety standards for human exposure were developed, a need was created for probes that could make an accurate, absolute measurement of electric fields with a wide range of parameters, such as the level, frequency, and polarization. A new generation of *E*-field probes was developed by government laboratories and commercial firms to meet this need. This paper presents the basic theory for these probes, describes several practical design that have been implemented, reviews the major applications of the probes, and discusses the state of the art of these devices, including developments which are likely to occur in the near future.

This paper was invited for publication by the IEEE Wave Propagation Standards Committee.

Manuscript received June 22, 1982; revised January 4, 1983. The portion of this work performed at the Georgia Institute of Technology was supported in part by the National Science Foundation under Grant ECS-8105163.

H. I. Bassen is with the Department of Health and Human Services, Food and Drug Administration, National Center for Devices and Radiological Health, Rockville, MD 20857.

G. S. Smith is with the School of Electrical Engineering, Georgia Institute of Technology, Atlanta, GA 30332.

For a comprehensive list of references on the design and use of electric field probes, the reader is referred to the extensive bibliography of reference [10].

II. BASIC PRINCIPLES OF OPERATION

Several electric field probes have been developed with a construction similar to that shown schematically in Fig. 1. These probes contain five basic elements: a dipole antenna, a nonlinear detector, optional lumped element shaping and filtering networks, a nonperturbing transmission line and monitoring instrumentation [2]-[10]. The operation of the probe is fairly simple. For a continuous-wave incident field with the frequency ω, the antenna produces an oscillating voltage across the detector at its terminals. Due to the nonlinear characteristics of the detector, a signal with a dc component proportional to the square of the amplitude of the incident field is developed at the detector. This signal is filtered, and the dc component is conveyed over the transmission line to the monitoring instrumentation. Thus, a signal proportional to the square of the amplitude of the incident field is measured.

In the brief analysis that follows, the simplified probe of Fig. 2(a) is used. The lumped element shaping and filtering networks are not included in this probe; the lossy transmission line connecting the detector to the monitoring instrumentation provides the low-pass filtering for the detector. The incident continuous-wave electric field, for simplicity, is assumed to be parallel to the axis of the dipole:

$$\vec{E}_z^{\,i}(\vec{r}, t) = E_z^i(\vec{r}) \cos [\omega t + \phi_z(\vec{r})]\hat{z}$$
$$= \text{Re } [\mathbf{E}_z^i(\vec{r}, \omega)e^{j\omega t}]\hat{z}, \tag{1}$$

where Re indicates the real part and bold type indicates a phasor quantity. A more general field will be considered later.

The incident electric field generally is not uniform along the axis of the dipole antenna (z axis). To provide spatial resolution of the field, the antenna is often made physically short and electrically short, $\beta_0 h = 2\pi h/\lambda_0 \ll 1$, where h is the half-length of the dipole and λ_0 is the wavelength in free space.[1] The voltage across the terminals of the electrically short dipole when they are open circuited is approximately proportional to the incident electric field at the center of the dipole (the origin O in Fig. 1):

$$V_{oc}(\omega) \approx h\mathbf{E}_z^i(0, \omega), \tag{2}$$

and the impedance of the driven dipole is approximately capacitive:

$$Z_A(\omega) \approx -j/\omega C_A = -j\zeta_0 [\ln (h/a_A) - 1]/\pi\beta_0 h, \tag{3}$$

where a_A is the radius of the dipole conductor and ζ_0 is the im-

[1] Spatial resolution is determined by the variation of the incident electric field over the length of the dipole. For high resolution, the length of the dipole must be small compared to the distance over which the gradient of the electric field is significant.

0018-926X/83/0900-0710$01.00

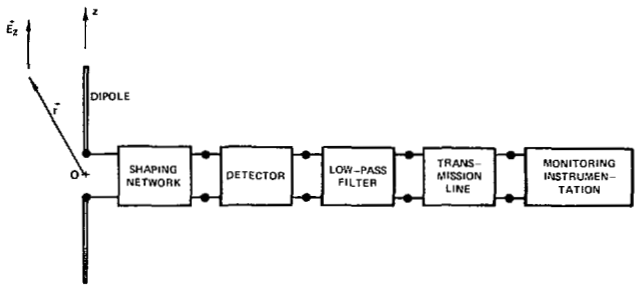

Fig. 1. Schematic of receiving probe.

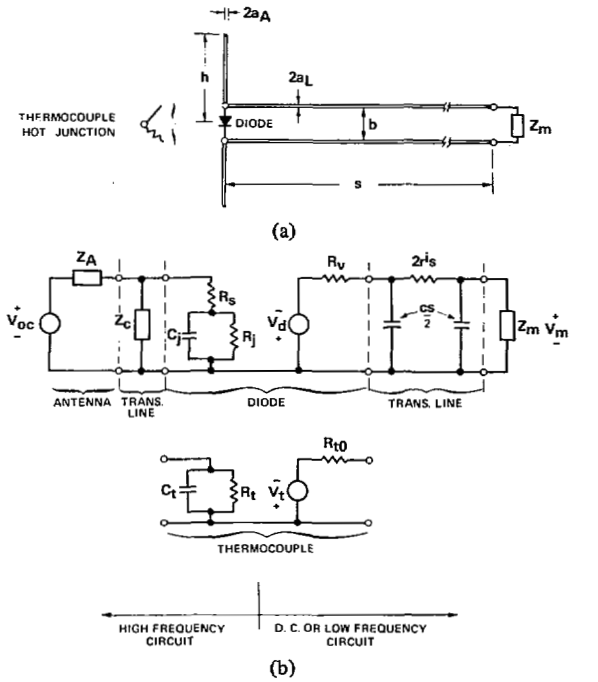

Fig. 2. (a) Simplified probe. (b) Equivalent circuit for probe with diode or thermocouple detector.

pedance of free space [11]. These two elements, the open circuit voltage and the antenna impedance, form the Thévenin equivalent circuit for the receiving dipole shown on the left of Fig. 2(b).

Detector

The detector in the probe is often an unbiased point contact or Schottky barrier diode operating in the square-law region, or a thermocouple junction. In Fig. 2(b) the equivalent circuit for the diode is divided into high and low-frequency sections. The high-frequency section consists of the junction resistance R_j and capacitance C_j, and the series resistance R_s; the parasitic elements associated with the packaging of the diode are omitted. The low-frequency circuit contains a voltage source V_d and the video resistance $R_v \approx R_s + R_j$. For square-law operation, the voltage source is proportional to the time average of the radio-frequency power absorbed by the diode [12], [13]:

$$V_d = \gamma_d P_d, \tag{4}$$

where γ_d is the voltage sensitivity of the diode.

For a thermocouple detector, the hot junction of the thermocouple with a series resistance R_t is placed across the terminals of the dipole; see the inset in Fig. 2(a). The series resistor may be a thin film of evaporated metal about 1000 Å thick forming the hot junction. The radio-frequency current through the resistor dissipates power P_t; this raises the temperature of the hot junction T_H above that of the cold junction T_C and produces a thermoelectric voltage V_T that is approximately proportional to the time-average power dissipated in the resistor:

$$V_t = \alpha(T_H - T_C) \approx \gamma_t P_t, \tag{5}$$

where α is the Seebeck coefficient for the particular combination of materials used in the thermocouple. The high-frequency section of the equivalent circuit for the thermocouple detector consists of the resistor R_t with possibly a parallel capacitance C_t to account for a change in the geometry at the junction. The low-frequency circuit contains the thermoelectric voltage source V_t and the series resistor R_{t0}. Note that due to frequency dependence, the resistance R_{t0} may not equal R_t.

Resistive Transmission Line

The transmission line connecting the detector to the monitoring instrumentation has an internal resistance per unit length r^i for each conductor and a capacitance per unit length c. The resistance per unit length is usually chosen to be much greater than the inductive reactance per unit length ($2r^i \gg \omega l$), making the characteristic impedance and wave-number on the line approximately

$$Z_c(\omega) = R_c + jX_c \approx \sqrt{\frac{r^i}{\omega c}}\,(1-j), \tag{6}$$

and

$$k_L(\omega) \approx \sqrt{r^i \omega c}\,(1-j). \tag{7}$$

In addition, the length of the line is selected so that the attenuation of a wave propagating over it will be large ($|\exp(-jk_L s)| \ll 1$) at all of the radio frequencies of interest. The high resistance per unit length of the transmission line produces three effects: it reduces the direct reception of the incident field by the line, it reduces the scattering of the incident field by the line, and it makes the line behave as a low-pass filter [14].

The transmission line can behave as a receiving antenna for the incident field and produce a signal at the detector; this will cause the field pattern for the probe to differ from that of the short dipole. The principal perturbations introduced are a shift in the position of the nulls in the elevation pattern for the dipole and a response to electric fields orthogonal to the axis of the dipole [14]. For a lossy two-wire line with a conductor spacing b, the relative distortion in the dipole pattern for a plane wave incident is approximately proportional to the dimensionless parameter

$$\chi = \frac{\ln(h/a_A) - 1}{\pi}(b/h)(\zeta_0/2r^i h). \tag{8}$$

Note that the parameter χ is quadratic in the dipole length h, but linear in both the spacing b and the resistance per unit length ($1/r^i$) of the transmission line conductors. Thus, the relative distortion is kept fixed while halving the dipole length either by decreasing the conductor spacing by a factor of four, or by increasing the conductor resistance by a factor of four.

When the probe is used in a multifrequency environment with widely separated frequency components, the reception by the transmission line may not be negligible at all of the frequencies. As an example, consider a probe being used to measure a high radio-frequency signal in close proximity to an electronic device. Any low-frequency ac fields produced by the device (interference

for the probe) will couple to the probe's transmission line. The filtering action of the resistive line may not be sufficient at the low frequency to suppress the propagation of the interference over the transmission line to the detector and to the monitoring instrumentation.

The current induced in the transmission line by the incident field produces a secondary or scattered field which also may be a source of error in the measurement. The reduction in the scattered field that results from the use of resistive conductors is illustrated in Fig. 3(a), where the normalized total scattering cross section of the line σ_L/λ_0^2 is shown as a function of the normalized resistance per unit length $\bar{r}^i = r^i\lambda_0/\zeta_0$. The incident field is a plane wave with the electric field parallel to the conductors, and the line is one wavelength long $s/\lambda_0 = 1.0$. The two regions marked on the graph represent typical resistances at a frequency of 1 GHz for a round carbon-Teflon conductor developed by the National Bureau of Standards ($a_L = 0.38$ mm, $r^i = 65.6$ KΩ/m) and thin metallic-film conductors ($r^i = 1 - 10$ MΩ/m) [5], [6]. From this graph, it is clear why the highly resistive transmission lines are often referred to as "transparent" to electromagnetic fields at high radio and microwave frequencies.

A transmission line with a high resistance per unit length is very dispersive. This is illustrated in Fig. 3(b) where the voltage transmission ratio $V(s)/V(0)$ is shown as a function of the frequency for 20 cm long lines made from carbon-Teflon and thin film conductors. The transmission line is seen to behave as a low-pass filter with little distortion occuring for signals with frequencies below the point where $|k_L s| = 1.0$. In the high-frequency equivalent circuit of Fig. 2(b), the input impedance of the transmission line appears across the diode; for a line with high loss ($|\exp(-jk_L s)| \ll 1$), this is approximately the characteristic impedance Z_c. In the low-frequency circuit, the transmission line is represented by a "Pi" low-pass filter network.

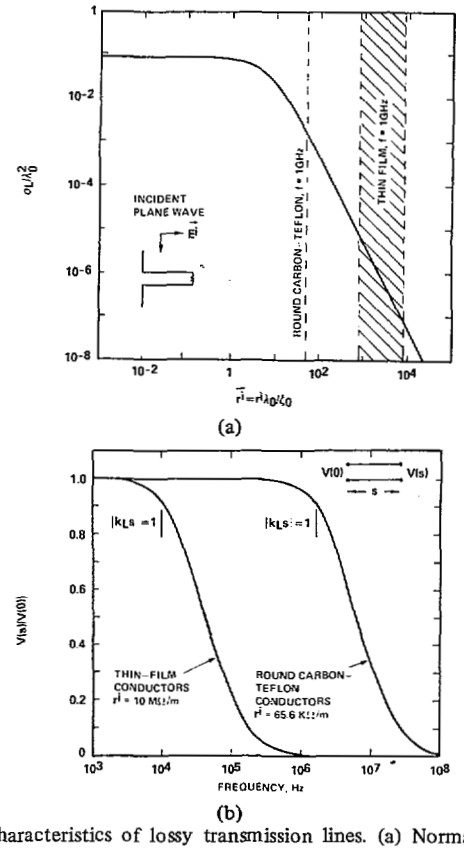

Fig. 3. Characteristics of lossy transmission lines. (a) Normalized total scattering cross section of a one wavelength long line $s/\lambda_0 = 1.0$ as a function of the normalized resistance per unit length. (b) The transmission line as a low-pass filter, $s = 20$ cm, $c = 20$ pF/m.

Probe Response

The response for the probe, i.e., the voltage V_m across the input impedance $Z_m = R_m + jX_m$ to the instrumentation, is easily determined from the equivalent circuit in Fig. 2(b).[2] The series resistance R_s is set equal to zero since it is often much smaller than the junction impedance; the response for a probe with a diode detector is then

$$|V_m| = \frac{R_m(\omega R_j C_A)^2 \gamma_d |V_{oc}|^2}{2R_j(R_m + R_v + 2r^i s)\{[1 + R_j R_c/|Z_c|^2]^2 + [\omega R_j(C_A + C_j) - R_j X_c/|Z_c|^2]^2\}}. \quad (9)$$

The same expression applies to a probe with a thermocouple detector when R_j, C_j, R_v, and γ_d are replaced by R_t, C_t, R_{t0}, and γ_t. Note that the capacitance of the elements in the "Pi" network of Fig. 2(b) and the reactance of the impedance Z_m do not appear in (9), since a dc signal is detected when the incident field is a continuous wave.

The lossy transmission line is usually designed to have an input impedance that is large compared to the impedance of the diode ($|Z_c| \gg R_j$). If this requirement cannot be satisfied by the transmission line alone, a lumped series resistance can be added to each conductor of the line to increase the impedance in parallel with the diode. With this approximation and (2), (9) simplifies to become

$$|V_m| = \gamma_d \left[\left(\frac{C_A}{C_A + C_j}\right)^2 \left(\frac{1}{1 + \omega_c^2/\omega^2}\right)\right] \cdot \left[\frac{h^2 |\mathbf{E}_z^i(0,\omega)|^2}{2R_j}\right]\left[\frac{R_m}{R_m + R_v + 2r^i s}\right] = C|\mathbf{E}_z^i(0,\omega)|^2 \quad (10a)$$

where

$$\omega_c = [R_j(C_A + C_j)]^{-1}. \quad (10b)$$

Each bracketed term in this equation is associated with elements in the equivalent circuit, Fig. 2(b). The first term accounts for the frequency dependent division of the antenna's open-circuit voltage V_{oc} between the antenna impedance and the diode impedance. The second term is the time-average of the radio-frequency power delivered to the diode when the diode impedance is large compared to the antenna impedance. The last term represents the division of the detected dc voltage V_d between the video resistance, the transmission line resistance and the resistance of the monitoring instrumentation.

The behavior of the response with frequency is shown in Fig.

[2] A complete discussion of the probe's respone, including the effects of parasitic elements in the diode equivalent circuit, is given in [11, ch. 3].

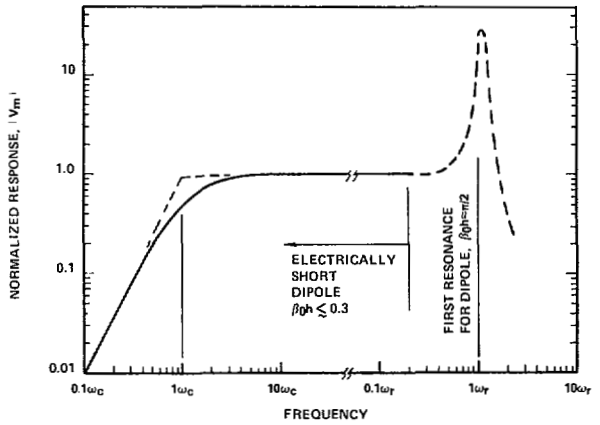

Fig. 4. Normalized response of probe versus frequency.

4; it is seen to have two distinct regions. Below the frequency ω_c the response approaches an asymptote which decreases as the square of the frequency (−12 dB/octave), and above ω_c the response approaches an asymptote which is independent of the frequency. This frequency dependence is easily understood by examining the voltage division between the elements in the high-frequency equivalent circuit of Fig. 2(b) and is discussed in detail in Section III-A.

When the frequency is increased beyond the point where the dipole antenna is electrically short ($\beta_0 h \gtrsim 0.3$), the elements in its equivalent circuit differ from the values in (2) and (3), and the response is no longer given by (10a). A typical response for the electrically longer antenna is shown as a dashed line in Fig. 4, and it is seen to peak in the vicinity of the frequency for the first resonance of the dipole ω_r (at ω_r, $\beta_0 h \approx \pi/2$). The response is relatively flat over the frequency range which extends from about $3\omega_c$ to $0.3\omega_r$. In practical designs, the resonant frequency ω_r is determined by the length of the dipole, and the frequency ω_c is changed mainly by adjusting the junction resistance R_j. Increasing R_j extends the region where the response is flat to lower frequencies; however, an increase in R_j also decreases the sensitivity of the probe (the output $|V_m|$ for a fixed field $|\mathbf{E}_z^i|$) unless the input resistance of the transmission R_m is large compared to the junction resistance. The factor γ_d is approximately proportional to R_j, and $R_v \approx R_j$; thus, the response (10a) is proportional to the frequency independent factor $R_m/(R_m + R_j + 2r^i s)$ when $\omega \gg \omega_c$. A change in the junction resistance R_j will not affect the sensitivity of the probe provided $R_m + 2r^i s \gg R_j$.

The preceding analysis is for a continuous-wave incident field. The response of a probe with a diode detector to an amplitude modulated incident field will be similar to (10a), provided the frequencies in the square of the modulating signal are within the pass band of the low-pass filter formed by the lossy transmission line, i.e., $|k_L s| \ll 1$ at these frequencies. A factor $f^2(t)$, where $f(t)$ is the modulating signal, must be included in (10a) in this event. For the result in (10a) to apply to the measurement of an amplitude modulated field with a thermocouple detector, the thermal time constant of the detector also must be short compared to the period of the highest frequency contained in the modulation.

Isotropic Probe

Consider the general monochromatic incident field expressed as the sum of three orthogonal components each of the form (1):

$$\vec{E}^i(\vec{r}, t) = \sum_{n=x,y,z} E_n^i(\vec{r}) \cos[\omega t + \phi_n(\vec{r})]\hat{n}$$

$$= \mathrm{Re}\left[\sum_n \mathbf{E}_n^i(\vec{r}, \omega) e^{j\omega t}\hat{n}\right]$$

$$= \mathrm{Re}\,[\vec{\mathbf{E}}^i(\vec{r}, \omega) e^{j\omega t}], \tag{12}$$

Each of the three orthogonal dipole probes shown in Fig. 5(a), when placed in this field, will have a response proportional to the square of the amplitude of a field component:

$$|V_m|_n = C|\mathbf{E}_n^i(0, \omega)|^2, \quad n = x, y, z. \tag{13}$$

After the three responses are summed, a signal proportional to the square of the Hermitian magnitude of the complex vector field $\vec{\mathbf{E}}^i(0, \omega)$ is obtained [15]:

$$\sum_n |V_m|_n = C \sum_n |\mathbf{E}_n^i(0, \omega)|^2 = C|\vec{\mathbf{E}}^i(0, \omega)|^2. \tag{14}$$

This signal is independent of the orientation of the probe with respect to the field; thus, the responses of the probe composed of the three orthogonal dipoles is isotropic. Note that the Hermitian magnitude of the complex field is an upper bound on the instantaneous field:

$$|\vec{E}^i(0, t)| \leqslant |\vec{\mathbf{E}}^i(0, \omega)|. \tag{15}$$

In practical field probes, the centers (terminals) of the three orthogonal dipoles generally are not coincident as in Fig. 5(a), but they are displaced from each other as in the configurations shown in Figs. 5(b), (c), and (d) [4], [5], [7]. Each dipole in Fig. 5(b) is mounted on a planar substrate; two of the dipoles make an angle of 45° and the third an angle of 90° with the long axis of the substrates. When the three substrates are combined in the "I-beam" configuration the dipoles are orthogonal. In Fig. 5(c), the dipoles are placed on planar substrates that are combined to form a tube whose cross section is an equilateral triangle. Each of the orthogonal dipoles makes an acute angle of 54.74° with the axis of the tube. The three axes of the orthogonal

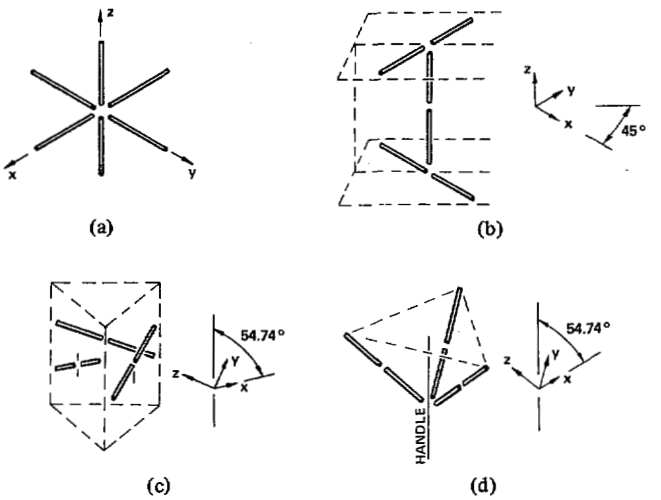

Fig. 5. (a) Three orthogonal dipoles with a common center. (b), (c), (d) Practical arrangements of three orthogonal dipoles with displaced centers.

dipoles in Fig. 5(d) are along the lateral edges of a regular pyramid whose base is an equilateral triangle. Each of the dipoles makes an acute angle of 54.74° with the altitude of the pyramid, and the handle of the probe is an extension of the altitude. When the centers of the dipoles are displaced, as in Figs. 5(b), (c), and (d), each probe measures a field component at a *different* position in space. The three components can be combined to estimate the Hermitian magnitude of the field at a single point (14) only if the field is assumed not to vary over the volume of space occupied by the dipoles. If the dipoles are physically and electrically short, this volume will also be physically and electrically small, and the assumption of a uniform field within the volume is justifiable.

When the electric field probe is used in inhomogeneous material media, such as biological tissue, the normalized response of the probe $|V_m|/|\mathbf{E}_z^i|^2$ may vary with position. For an electrically short dipole, this variation is mainly due to the change in the impedance of the antenna Z_A with a change in the electrical constitutive parameters of the material surrounding the probe. The variation can be reduced by making the antenna impedance small compared to the impedance of the detector ($C_A \gg C_j$ in the region where the resonse is flat) or by minimizing the variation in the antenna impedance by insulating the dipole [11], [16], [17]. The insulated dipole is formed by coating the antenna with a material whose relative dielectric constant ϵ_{ri} is lower than that of the surrounding medium ϵ_r. The impedance of the insulated dipole is fairly insensitive to variations in the electrical parameters of the surroundings; this is illustrated in Fig. 6, where the capacitance of a particular electrically short insulated dipole is seen to have little variation with ϵ_r once $\epsilon_r/\epsilon_{ri} \gtrsim 5$.

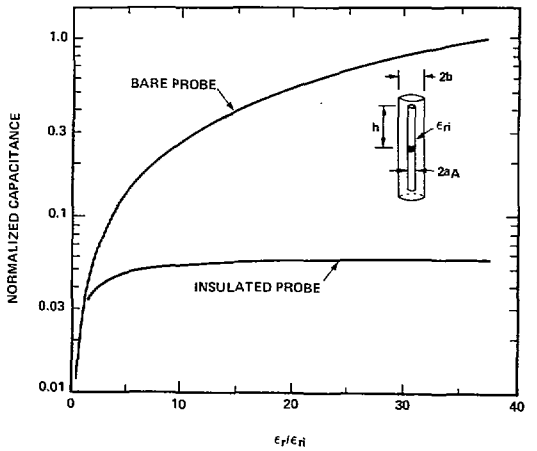

Fig. 6. Normalized capacitance of bare and insulated electrically short dipoles in medium with relative dielectric constant ϵ_r, $h/a = 18$, $b/a = 2.3$, $\epsilon_{ri} = 2.1$, $h/\lambda_0 = 3.7 \times 10^{-3}$.

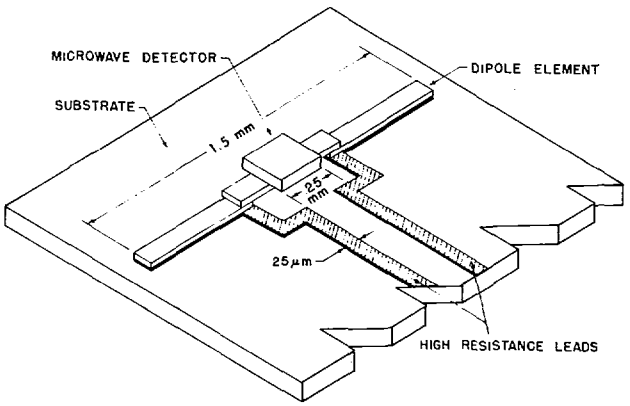

Fig. 7. Detail of dipole/detector for miniature *E*-field probe.

III. IMPLEMENTATION

A. Probes with Diode Detectors

The basic design of this device has been optimized by the U.S. National Bureau of Standards (NBS) [10] for coverage over the frequency ranges 0.2 to 1000 MHz.[3] Square-law response (output voltage proportional to $|\vec{E}^i|^2$) over the range from about 1 V/m to 2000 V/m (rms) is provided by using electronic circuitry which compensates for the nonsquare-law response of the diode detector at high output voltage levels (greater than about 25 mV). An array of three orthogonal dipoles, each of total length $2h = 1$ cm, is used to provide isotropic response. This is achieved by placing each dipole on a dielectric substrate, and combining three of the substrates to form a triangular support frame and handle, as in Fig. 5(c).

The use of a beam-lead carrier package for the Schottky diode chip minimizes detector parasitic inductance, to provide a flat nonresonant frequency response over a wide portion of the RF/microwave frequency range. A high resistance transmission line (low-pass filter) is formed by a sandwich arrangement which uses two flat thin carbon impregnated Teflon strips, with a resistance per unit length of about 4 MΩ/m, attached to a thin insulating double-sided adhesive tape. This probe is used in free space for both radiation hazard measurements and for electromagnetic compatibility measurements, with a standard shielded cable or another lossy transmission line connecting the probe to an electronic "readout box."

The National Center for Devices and Radiological Health (formerly the Bureau of Radiological Health (BRH)) and its contractors have developed miniaturized versions of the above probe using thin-film technology. The intended application of these miniature *E*-field probes is primarily for implantation in living animals or models used in biological effects studies [18]. These probes are constructed, as shown in Fig. 7, from a diode chip with integral beam leads and a dipole antenna of total length $2h = 1.5$ mm. The conductors of the lossy parallel wire transmission line are made of highly resistive thin-film material. Each dipole probe is mounted on a dielectric substrate, and three substrates are combined to form a tube of triangular cross section, as shown in Fig. 5(c). The array of three dipoles forms an isotropic probe. The tip of the probe is encapsulated in a dielectric material. The substrate and the encapsulation serve as insulation on the dipole antennas and help to make the probe's response independent of the electrical parameters of the surrounding medium when the probe is used in a material with a high dielectric constant, like biological tissue.

Square-law detection of *E*-fields is accomplished by limiting the RF voltage applied to the diode; this is a fortunate consequence of making the electrical length of the dipole very small. Other means of shaping the detected voltage versus RF field strength (such as the use of electronic circuitry, either analog or digital) are not necessary.

[3] A commercial firm, Holaday Industries, Edina, MN, has adapted the NBS design by adding resistance to the dipole elements and using a glass-packaged diode. The resultant device covers the frequency range 0.5 to 6000 MHz.

The diodes in the probe are selected so that their junction resistance R_j (see the equivalent circuit of Fig. 2(b)) is large enough to appear as an open circuit in comparison to the antenna impedance Z_A at high radio frequencies ($\omega \gg \omega_c$) The total open-circuit voltage of the antenna V_{oc} then appears across the diode, and the response of the probe with frequency is flat, as seen Fig. 4. Since the antenna impedance is primarily capacitive (the capacitance is about 0.1-0.2 pF), it increases with decreasing frequency, and at low radio frequencies eventually is greater than the diode impedance. The open circuit voltage of the antenna is then divided between the antenna impedance and the diode impedance, and the response of the probe decreases with decreasing frequency (the −12 dB/octave decrease that occurs at frequencies below ω_c in Fig. 4). The larger the value of the junction resistance, the lower the frequency ω_c at which the probe response begins to roll off. The junction resistance, however, cannot be increased indefinitely, since the video resistance of the diode R_v increases with the junction resistance ($R_v \approx R_j + R_s$). When the video resistance becomes large compared to the resistance of the metering instrumentation R_m, an insufficient amount of the detected voltage V_d will appear across the instrumentation. The net result is that the "high-impedance zero-bias" diodes or "medium barrier" Schottky diodes in the miniature E-field probe are chosen to have an optimal junction resistance, i.e., one large enough to produce sufficient bandwidth (low ω_c), yet not so high as to significantly decrease the sensitivity (R_j not large compared to R_m). Use of the optimal detector diode provides a flat frequency response for the probe over the range from 100 MHz to beyond 12 GHz and a sensitivity which enables measurement of field strengths of a few V/m.

The lossy transmission line, which is about 30 cm long in this probe, is connected to a telemetry system. This system contains a preamplifier that drives an analog to digital converter (voltage-controlled oscillator); the output of the converter modulates a light emitting diode producing optical data pulses that are transmitted over a fiber optic to a remote readout, see Fig. 8 [19]. The battery-operated three channel telemetry system is housed in a metal cube with sides of approximately 3 cm in length. Scattering errors introduced by the telemetry unit are less than about 0.25 dB, when the probe is in free space.

A recent paper describes a broad-band (200 KHz-26 GHz) probe with diode detectors developed by a commercial firm [9].[4] The three dipoles in this probe are each of length $2h = 3.2$ cm. Resistive strips carry the detected signal from the Schottky-barrier diodes at the terminals of the dipoles to the monitoring instrumentation. The broad-band response of the probe is obtained by making the dipoles from resistive thin film and including a shaping network at their terminals. Note that the dipoles of this probe are electrically long at the upper frequencies in its specified range of use ($2h \cong 2.8\lambda_0$ at 26 GHz). Thus, unlike the electrically short dipoles discussed earlier, the response of this probe will be a weighted average of the field over the length of the dipoles whose centers may be displaced by a few wavelengths at the higher frequencies.

B. Probes with Thermocouple Detectors

Several isotropic E-field probes with thermocouple detectors have been developed for use over consecutive frequency bands, which when combined cover the entire frequency range of 10 MHz to 26 GHz [3], [4].[5] In one probe, three antennas, each being several centimeters long, are arranged in the orthogonal array shown in Fig. 5(d). For broad-band response each antenna is formed from many antimony-bismuth thermocouples (detectors) distributed along a hairpin curve, see Fig. 9(a). Note that the hot junctions of the thermocouples, Fig. 9(b), are formed by decreasing the cross section of the conductors; this increases the electrical resistance and the power dissipation at these points. The resulting antenna/detector of this probe is relatively inefficient and does not perturb the field being measured. The low sensitivity is compensated for by providing a low-noise preamplifier in the handle. A parallel wire transmission line with tapered resistive thin-film conductors connects the antennas with the preamplifier.

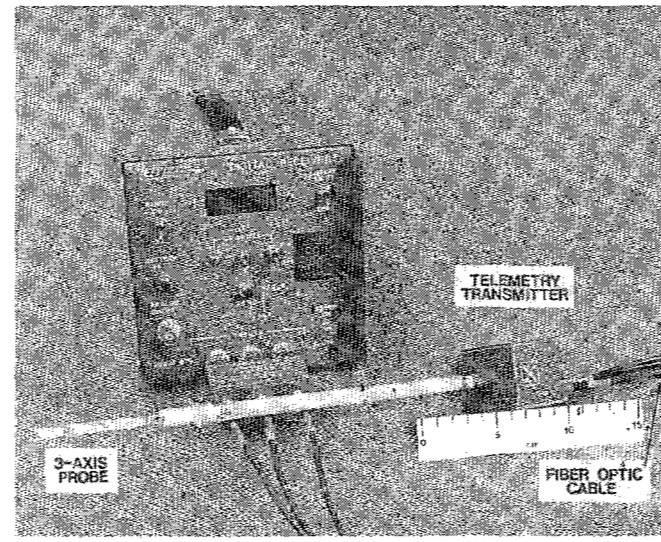

Fig. 8. E-Field probe with optical telemetry system.

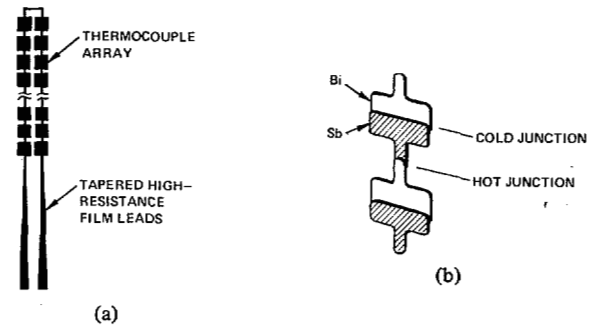

Fig. 9. (a) Antenna element formed from thermocouple array. (b) Detail of thermocouples.

Each array of thermocouple elements in this probe is not electrically short at the upper end of the frequency range specified for its use. Thus, this probe will not necessarily give an accurate indication of the electric field at a point, but a weighted average of the field over the length of the array.

The primary advantage of the thermocouple probe is its inherent ability to integrate, via thermal means, pulsed high level E-fields, such as those in the vicinity of a radar transmitter. The short duration of these pulses (microseconds) precludes the use of dipole/diode probes. This is due to the wide bandwidth of the pulses compared to the narrow bandwidth of the resistive trans-

[4] General Microwave Corp., Farmingdale, NY 11725.

[5] Narda Microwave Corp., Hauppauge, NY 11788.

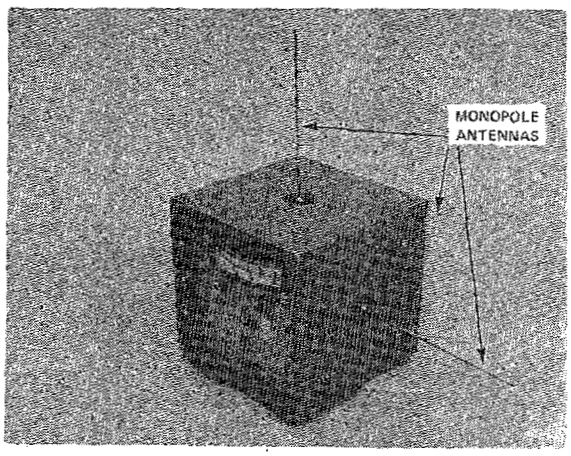

Fig. 10. *E*-field probe with active electronics.

mission line (low-pass filter) which must carry the detected signal from the diode to the processing circuitry where integration would occur.

C. Probes with Active Detector Circuitry

Probes that have active detection circuitry at the terminals of the dipoles were developed by the U.S. National Bureau of Standards [20], [21]. A commercial system is now available for use in the frequency range 0.01 to 220 MHz.[6] The active circuitry, a high impedance RF amplifier, is used to properly terminate the short monopoles (less than 10 cm in length) and obtain a flat frequency response in the low-frequency portion of the usable range. In this device, orthogonal monopoles are used to obtain isotropic response. The active circuitry, batteries and readout meter are housed in a cube with sides 10 cm in length. The metal cube also serves as a quasi-image plane for the monopole antennas, as shown in Fig. 10. The above system also includes a fiber optic data link from the cube to the remote instrumentation. The fiber optic link is driven by a voltage-controlled oscillator and a light emitting diode housed in the metal cube. Good linearity, frequency response, and antenna patterns have been obtained in laboratory tests of this device over the frequency range 10 to 100 MHz [22].

D. Summary of E-Field Probe Performance Parameters

Table I presents data on the critical parameters of the probes which were discussed previously; all of the probes use three orthogonal elements to obtain isotropic response.

IV. APPLICATIONS OF *E*-FIELD PROBES

The primary application of *E*-field probes is in the assessment of radiation hazards. United States RF/microwave safety standards limit human exposure at frequencies ranging from 300 kHz to 100 000 MHz to levels ranging from 60 V/m to 600 V/m (rms). For most radiation-safety surveys, a probe with an array of three small dipoles is used, since the polarization of the fields being measured is unknown, particularly for complex near-field radiation situations [23]. The uncertainty of measurement for this type of probe when all sources of error are considered can approach ±2 dB [22], [24].

[6] Instruments for Industry, Farmingdale, NY 11735.

TABLE I

Type of Probe	Frequency Range, MHz	Dynamic Range, V/m (RMS)	Approximate Antenna Size, cm*
Dipole/Diode	0.5 to 6000	1 to 3000	2
Miniature Dipole/Diode	100 to 12,000	10 to 200	0.3
Resistive Dipole/Diode	0.2 to 26,000	2 to 275	3
Thermocouple/ Dipole	10 to 3000 300 to 26,000	80 to 2750 10 to 275	10 5
Monopole with Active RF Detector	0.01 to 220	1 to 1000	10 to 15**

*Maximum dimension of total array.
**Including metallic circuit housing.

E-field probes have been used frequently for *external* (exposure) field mapping in biological effects studies involving animals that are purposely exposed to electromagnetic fields [25]. Miniature implantable *E*-field probes also have been used in several studies to *internally* probe living or sacrificed animals to ascertain the electric field in specific organs when the animal is exposed to RF/microwave radiation [18]. The measurement uncertainty associated with the implantable *E*-field probe may approach ±2 to ±3 dB if the relative dielectric constant of the medium is above 5.

With the implantable *E*-field probe, an animal is typically exposed to electromagnetic radiation with a power density of 1 to 10 mW/cm^2. The 3 mm diameter probe tip measures the three orthogonal *E*-field vector components at the selected site. Internal dosimetric methods other than the *E*-field probe have almost universally been thermal in nature, involving exposures of an animal to intense radiation ($>$ 100 mW/cm^2), followed by measurements of the temperature rise at various points in the animal [26]. The electric field is computed from the temperature rise by using the relationship:

$$\mathrm{SAR} = \tfrac{1}{2}\,\sigma\,|\vec{\mathbf{E}}|^2/\rho = c\,\frac{\Delta T}{\Delta t} \tag{16}$$

where

- SAR Specific Absorption Rate (W/kg).
- $|\vec{\mathbf{E}}|$ Hermitian magnitude of the internal peak electric field (V/m).
- σ Effective electrical conductivity of the tissue at the point of measurement, and at the frequency of the exposure field (S/m).
- ρ Mass density of the tissue (kg/m^3).
- ΔT Temperature rise (°C).
- Δt Duration of exposure (s).
- c Specific heat of the tissue (J/kg°C).

From the above equation it is easily seen that the measurement of the electric field strength in a biological specimen using a thermal probe, as compared to a well designed *E*-field probe, is much more involved and requires much more specific information about the exposure and the electrical and thermal parameters of the tissue at the point of measurement. Conversely, measurement of the specific absorption rate with an *E*-field probe requires knowledge of the conductivity and the density of the tissue.

E-field probes have also been used to map the near-field of RF/microwave emitting therapy devices, such as microwave and shortwave diathermy systems (used to treat muscular and connec-

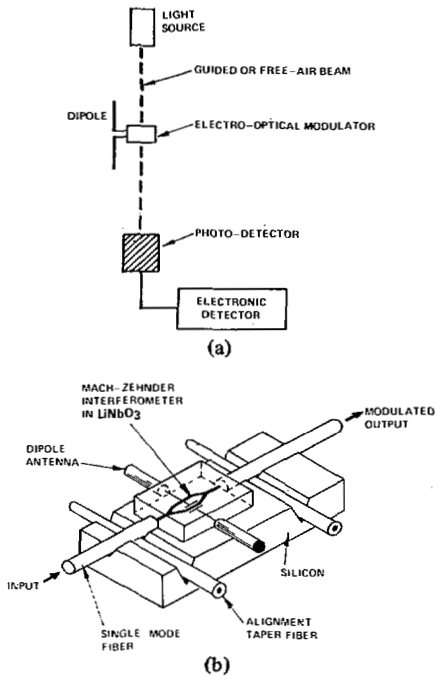

Fig. 11. (a) Electric field measurement system using electro-optical modulator. (b) Antenna/integrated optical modulator.

tive tissue injuries) and microwave hyperthermia systems for cancer treatment [27]. Measurements have been made of the individual vector components of the E-field which lie in a plane parallel and very close (5 to 25 mm) to the aperture of a diathermy applicator [28]. These results are used to predict the relative efficiency of the applicator and the pattern of energy deposition in planar models of the human tissue.

Another application of E-field probes is assessing the electromagnetic compatibility of electronic devices. For example, E-field probes are used to monitor the field strengths in the proximity of electronic devices which are susceptable to RF interference, such as sensitive medical monitoring equipment (electroencephalographic (EEG) devices).

V. FUTURE ADVANCES IN E-FIELD PROBE TECHNOLOGY

In an effort to reduce the size of the three-axis implantable probe, a dipole/diode integrated circuit is being developed with individual dipole antennas of total length $2h \approx 0.6$ mm [29]. Special techniques are being used to produce a diode chip that is electrically and mechanically compatible with the electrically small antenna. The production of an isotropic probe containing three dipoles with an outer diameter of 1–2 mm is this program's goal.

An electrically small dipole may be coupled to an optical modulator so that the RF voltage developed by the antenna causes a direct, instantaneous change in the amplitude of a beam of light passing through the modulator [30], see Fig. 11(a). This passive technique provides isolation of the probe's antenna, just as the high resistance lossy transmission lines do in present E-field probes. The optical technique has the additional advantage that it also provides a very fast response time (less than one cycle of the RF field) and phase measurement capabilities. The lossy transmission line, with its inherent low-pass filtration, cannot provide similar performance. The system shown in Fig. 11(b) uses an integrated optical modulator coupled to a laser diode through a single-mode optical fiber. Such a modulator has been designed for use with a 3 cm long dipole [31]. A flat frequency response from one to several hundred MHz is the design goal, with reproduction of the instantaneous (RF) waveform occurring at a remote site where the optical fiber is coupled to a photodiode detector.

VI. CONCLUSION

Electric field probes have been developed and used over much of the RF/microwave spectrum. Probes are commercially available for near and far zone isotropic measurements of the magnitude of the electric field both in free space as well as in material media, such as within living animals used in biological effects studies. In complex near-zone fields, only those probes whose maximum dimension is a small fraction of a wavelength can be expected to give a reading that approaches the value of the field at a point. Radiation hazard and electromagnetic compatibility surveys make use of broad-band E-field probes which yield uncertainties of 1 to 3 dB when used in complex near field environments. New technologies will improve the performance and reduce the size of E-field probes and will enable them to be applied in other areas.

REFERENCES

[1] C. L. Andrews, "Diffraction pattern in a circular aperture measured in the microwave region," *J. Appl. Phys.*, vol. 21, pp. 761–767, Aug. 1950.
[2] A. W. Rudge, "An electromagnetic radiation probe for near-field measurements at microwave frequencies," *J. Microwave Power*, vol. 5, pp. 155–174, Nov. 1970.
[3] E. E. Aslan, "Electromagnetic radiation survey meter," *IEEE Trans. Instrum. Meas.*, vol IM-19, pp. 368–372, Nov. 1970.
[4] ——, "Broad-band isotropic electromagnetic radiation monitor," *IEEE Trans. Instrum. Meas.*, vol. IM-21, pp. 421–424, Nov. 1972.
[5] R. R. Bowman, "Some recent development in the characterization and measurement of hazardous electromagnetic fields," in *Biological Effects and Health Hazards of Microwave Radiation*. Warsaw, Poland: Polish Medical Publishers, 1974, pp. 217–227.
[6] F. Greene, "Development of electric and magnetic near field probes," Nat. Bur. Stand. Tech. Note 658, Jan. 1975.
[7] H. Bassen, M. Swicord, and J. Abita, "A miniature broad-band electric field probe," *Annals of the New York Academy of Sciences, Biological Effects of Nonionizing Radiation*, vol. 247, pp. 481–493, Feb. 1975.
[8] H. Bassen, W. Herman, and R. Hoss, "EM probe with fiber optic telemetry," *Microwave J.*, vol. 20, pp. 35–39, Apr. 1977.
[9] S. Hopfer and Z. Adler, "An ultra broad-band (200 kHz–26 GHz) high-sensitivity probe," *IEEE Trans. Instrum. Meas.*, vol. IM-29, pp. 445–451, Dec. 1980.
[10] E. B. Larson and F. X. Ries, "Design and calibration of the NBS isotropic electric-field monitor (EFM-5), 0.2 to 1000 MHz," Nat. Bur. Stand. Tech. Note 1033, Mar. 1981.
[11] R. W. P. King and G. S. Smith, *Antennas in Matter: Fundamentals, Theory and Applications*. Cambridge, MA: M.I.T. Press, 1981, ch. 3.
[12] A. Uhlir, Jr., "Characterization of crystal diodes for low-level-microwave detection," *Microwave J.*, vol. 6, pp. 59–67, July 1963.
[13] H. A. Watson, *Microwave Semiconductor Devices and Their Applications*. New York: McGraw-Hill, 1969, ch. 12.
[14] G. S. Smith, "Analysis of miniature electric field probes with resistive transmission lines," *IEEE Trans. Microwave Theory Tech.*, vol. MTT-29, pp. 1213–1224, Nov. 1981.
[15] P. F. Wacker and R. R. Bowman, "Quantifying hazardous electromagnetic fields: Scientific basis and practical considerations," *IEEE Trans. Microwave Theory Tech.*, vol. MTT-19, pp. 178–187, Feb. 1971.

[16] G. S. Smith, "A comparison of electrically short bare and insulated probes for measuring the local radio frequency electric field in biological systems," *IEEE Trans. Biomed. Eng.*, vol. BME-22, pp. 477–483, Nov. 1975.
[17] ——, "The electric-field probe near a material interface with application to the probing of fields in biological bodies," *IEEE Trans. Microwave Theory Tech.*, vol. MTT-27, pp. 270–278, Mar. 1979.
[18] H. Bassen, P. Herchenroeder, A. Cheung, and S. Neuder, "Evaluation of an implantable electric-field probe within finite simulated tissues," *Radio Sci.*, vol. 12, pp. 15–25, Nov./Dec. 1977.
[19] H. Bassen and R. Hoss, "An optically linked telemetry system for use with electromagnetic field measurement probes," *IEEE Trans. Electromagn. Compat.*, vol. EMC-20, pp. 483–488, Nov. 1978.
[20] F. Greene, "A new near zone electric field strength meter," Nat. Bur. Stand. Tech. Note 345, Nov. 1966.
[21] E. Larsen, J. Andrews, and E. Baldwin, "Sensitive isotropic antenna with fiber optic link to a conventional receiver," Nat. Bur. Stand. Rep. NBSIR 75-819, Sept. 1976.
[22] B. Nesmith and P. Ruggera, "Performance evaluation of RF electric and magnetic field measuring instruments," Bur. Radiological Health, Food and Drug Administration, Rockville, MD, Publication FDA 82-8185, Mar. 1982.
[23] "Safety levels with respect to human exposure to radio frequency electromagnetic fields, 300 KHz to 10 GHz," Amer. Nat. Stand. C95.1-1982, IEEE, Piscataway, NJ.
[24] "Recommended practice for the measurement of hazardous electromagnetic fields–RF and microwave," Amer. Nat. Stand. C95.5-1981, IEEE, Piscataway, NJ.
[25] S. Oliva and G. Catravas, "A multiple-animal array for equal power density microwave irradiation," *IEEE Trans. Microwave Theory Tech.*, vol. MTT-25, pp. 433–436, May 1977.
[26] C. Johnson and A. Guy, "Nonionizing electromagnetic wave effects in biological materials and systems," *Proc. IEEE*, vol. 60, pp. 692–718, June 1972.
[27] J. Lehmann, J. Stonebridge, and A. Guy, "A comparison of patterns of stray radiaton from therapeutic microwave applicators measured near tissue-substitute models of human subjects," *Radio Sci.*, vol. 14, pp. 271–283, Nov./Dec. 1979.
[28] G. Kantor, D. Witters, and J. Greiser, "The performance of a new direct contact applicator for microwave diathermy," *IEEE Trans. Microwave Theory Tech.*, vol. MTT-26, pp. 563–568, Aug. 1978.
[29] G. Gimpleson and T. Batchman, "Material problems in the construction of a media independent radiation probe," in *Conf. Proc. IEEE Southeastcon '81*, pp. 820–824, Apr. 1981.
[30] H. Bassen and R. Peterson, "Antenna with electro-optic modulator," U.S. Patent 4 070 621, Jan. 1978.
[31] H. Bassen, C. Bulmer, and W. Burns, "A field-strength measurement system using a linear integrated optical modulator," in *IEEE Int. Symp. Digest*, Aug. 1980.

Howard I. Bassen (M'77–SM'78) received the B.S.E.E. degree from the University of Maryland, College Park, in 1965. From 1965 to 1970, he completed a variety of graduate courses in electrical engineering at George Washington University, Washington, DC, and Catholic University, Washington, DC. He received the M.S. degree in administration (Administration of Science and Technology) from George Washington University.

From 1965 to 1970 he performed RF and microwave antenna design and radar systems research at the U.S. Army's Harry Diamond Laboratories. From 1970 to 1972, he served as project engineer with the U.S. Postal Service Laboratory, developing both electromagnetic and X-ray weapon detection systems. He is currently the Chief of the Electromagnetics Branch in the Food and Drug Administration's National Center for Devices and Radiological Health. Since 1972 he has been involved in microwave hazard instrument development and calibration. In addition, he is responsible for the direction of laboratory research and development programs associated with medical devices utilizing electromagnetic fields including cancer hyperthermia and diathermy.

Mr. Bassen is a member of the American National Standards Commiteee C95 (electromagnetic radiation hazard and measurement standards) and the ANSI C63 Committee (electromagnetic compatibility). He is a member of the IEEE Bioelectromagnetics Society. He holds two patents on antenna systems.

Glenn S. Smith (S'65–M'72–SM'80) was born in Salem, MA, on June 1, 1945. He received the B.S.E.E. degree from Tufts University, Medford, MA, in 1967 and the S.M. and Ph.D. degrees in applied physics from Harvard University, Cambridge, MA, in 1968 and 1972, respectively.

From 1969 to 1972 he was a Teaching Fellow and Research Assistant in Applied Physics at Harvard University. From 1972 to 1975 he served as a Postdoctoral Research Fellow at Harvard University and also as a part-time Reseach Associate and Instructor at Northeastern University, Boston, MA. He is currently an Associate Professor of Electrical Engineering at Georgia Institute of Technology, Atlanta.

Dr. Smith is a member of Tau Beta Pi, Eta Kappa Nu, Sigma Xi, and Commission B of the International Union of Radio Science. He is co-author with R. W. P. King of the book *Antennas in Matter: Fundamentals, Theory and Applications*.